Optical Boron Nitride Insulator Erosion Characterization of a 200 W Xenon Hall Thruster

William A. Hargus, Jr.
Joshua Strafaccia
Air Force Research Laboratory
Spacecraft Propulsion Branch
Edwards AFB, CA 93524

Abstract

Vacuum ultraviolet emission (137.9 nm) of boron neutrals sputtered from a 200 W xenon Hall thruster boron nitride insulator is evaluated as a diagnostic for real time evaluation of thruster insulator erosion. Three Hall thruster plasma control variables are examined; ion energy (discharge potential), ion flux (propellant flow), and plasma conductivity (magnetic field strength). The boron emission, and hence the insulator erosion rate, varies linearly with ion energy and ion flux. A minimum erosion rate appears at intermediate magnetic field strengths. This may indicate that local plasma conductivity significantly affects the divergence of the plasma plume and hence thruster lifetime. The emission measurements of insulator erosion are supported by near field (~10 mm) xenon ion laser induced fluorescence velocity measurements which confirm that changes in the magnetic field produce significant changes in the ion flow vectors. The near field plume appears to be relatively invariant to changes in the plasma density, but increased flow divergence may be attributed to changes in magnetic strength. Faraday probe plume divergence measurements in the far field (60 cm) show that some of these differences propagate into the far field.

Introduction

Hall thruster lifetime is determined by the erosion of the boron nitride (BN) dielectric insulator surrounding the acceleration channel. Divergent ionized xenon propellant sputters the channel walls. Larger thrusters (>1 kW) have lifetimes approaching 10^4 hours. Smaller thrusters have shorter lifetimes due to plasma/geometrical scaling requirements which increase ion current density in the discharge as well as radial magnetic field divergence.

The goal of this study is to examine the use of optical emission from the thruster plasma, specifically emission from boron (B) sputtered from a protruding central BN covered pole piece, to determine the effect of various operating conditions on thruster lifetime. Due to the geometry of the thruster being studied, the measured erosion is in the near plume where the majority of the ion acceleration has previously occurred and the local number densities are low. It is therefore implicitly assumed that the emission of B is proportional to the sputter rate of insulator material. This is a different approach than taken by other researchers. It is believed that since the B emission studied in this effort is in the low density plume region, that more complex analysis is not required.

The emission measurements are supported by laser-induced fluorescence (LIF) xenon ion velocity measurements. These provide information on the near field ion velocities and determine some of the properties of the ions which produce the BN erosion of the central magnetic pole. Faraday probe measurements taken 60 cm from the thruster complement these two sets of measurements and show how the changes in operating conditions propagate into the far field. Additionally, the Faraday probe measurements provide a measure of the ion current and the extent to which it is affected due to changes in operating conditions.

The motivation for this effort is the need for a diagnostic to characterize the effects of thruster (in particular the Busek BHT-200-X3) operation on life. It

Report Documentation Page

Form Approved
OMB No. 0704-0188

1. REPORT DATE	2. REPORT TYPE	3. DATES COVERED
MAY 2005		**-**

4. TITLE AND SUBTITLE	5a. CONTRACT NUMBER
Optical Boron Nitride Insulator Erosion Characterization of a 200 W Xenon Hall Thruster	5b. GRANT NUMBER
	5c. PROGRAM ELEMENT NUMBER
6. AUTHOR(S) **William Hargus, Jr.; Joshua Strafaccia**	5d. PROJECT NUMBER **2308**
	5e. TASK NUMBER **0535**
	5f. WORK UNIT NUMBER
7. PERFORMING ORGANIZATION NAME(S) AND ADDRESS(ES) **Air Force Research Laboratory (AFMC),AFRL/PRSS,1 Ara Road,Edwards AFB,CA,93524-7013**	8. PERFORMING ORGANIZATION REPORT NUMBER
9. SPONSORING/MONITORING AGENCY NAME(S) AND ADDRESS(ES)	10. SPONSOR/MONITOR'S ACRONYM(S)
	11. SPONSOR/MONITOR'S REPORT NUMBER(S)

12. DISTRIBUTION/AVAILABILITY STATEMENT
Approved for public release; distribution unlimited

13. SUPPLEMENTARY NOTES

14. ABSTRACT

Vacuum ultraviolet emission (137.9 nm) of boron neutrals sputtered from a 200 W xenon Hall thruster boron nitride insulator is evaluated as a diagnostic for real time evaluation of thruster insulator erosion. Three Hall thruster plasma control variables are examined; ion energy (discharge potential), ion flux (propellant flow), and plasma conductivity (magnetic field strength). The boron emission, and hence the insulator erosion rate, varies linearly with ion energy and ion flux. A minimum erosion rate appears at intermediate magnetic field strengths. This may indicate that local plasma conductivity significantly affects the divergence of the plasma plume and hence thruster lifetime. The emission measurements of insulator erosion are supported by near field (~10 mm) xenon ion laser induced fluorescence velocity measurements which confirm that changes in the magnetic field produce significant changes in the ion flow vectors. The near field plume appears to be relatively invariant to changes in the plasma density, but increased flow divergence may be attributed to changes in magnetic strength. Faraday probe plume divergence measurements in the far field (60 cm) show that some of these differences propagate into the far field.

15. SUBJECT TERMS

16. SECURITY CLASSIFICATION OF:			17. LIMITATION OF ABSTRACT	18. NUMBER OF PAGES	19a. NAME OF RESPONSIBLE PERSON
a. REPORT **unclassified**	b. ABSTRACT **unclassified**	c. THIS PAGE **unclassified**		**10**	

appears that relatively small changes in thruster operating conditions result in measurable changes in the divergence of the ionized propellant flow. This study attempts to determine how these changes can be determined and correlated using laboratory diagnostics.

Apparatus and Experiment

Test Facility and Hall Thruster

The measurements presented in this work were performed in Chamber 6 at the Air Force Research Laboratory (AFRL) Electric Propulsion Laboratory at Edwards AFB, CA. Chamber 6 is a nonmagnetic stainless steel chamber with a 1.8 m diameter and 3.0 m length. It has a measured pumping speed of 32,000 l/s on xenon. Pumping is provided by four single stage cryo-panels (APD single stage cold heads at ~25 K) and one 50 cm two stage APD cryo-pump (<12 K). Chamber background pressure during thruster operation is approximately $5x10^{-6}$ Torr, corrected for xenon.

Figure 1 shows the thruster used in this investigation. It is the Busek Company BHT-200-X3 200W Hall thruster which has been described in detail elsewhere [1]. Table 1 shows the nominal thruster operating condition. During thruster operation, these parameters are monitored and recorded at 1 Hz.

Table 1: Nominal Thruster Operating Conditions

Anode flow	840 μg/s (Xe)
Cathode flow	98 μg/s (Xe)
Anode potential	250 V
Anode current	0.85 A
Keeper current	0.5 A
Magnet current	1.0 A
Heater current	3.0 A

Due to the placement of the central magnetic pole, the BHT-200 Hall thruster provides an excellent opportunity to study the process of insulator erosion. The pole and its BN cover protrude approximately 7 mm from the front face (exit plane) of the thruster. This *nose cone* is in the path of a portion of the divergent ionized xenon plume and is subject to erosion in an optically accessible location.

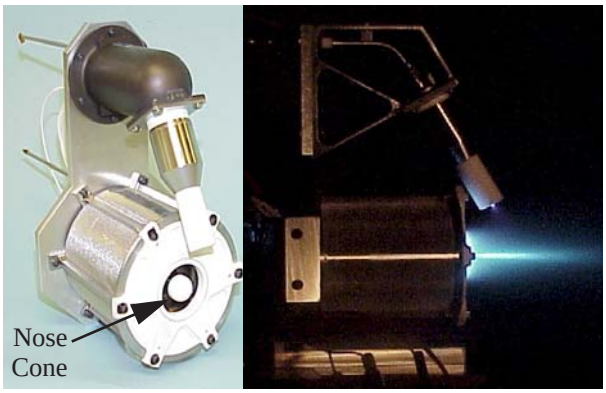

Fig. 1. Busek BHT-200-X3 Hall thruster. Note the center magnetic pole covered by a boron nitride nose cone.

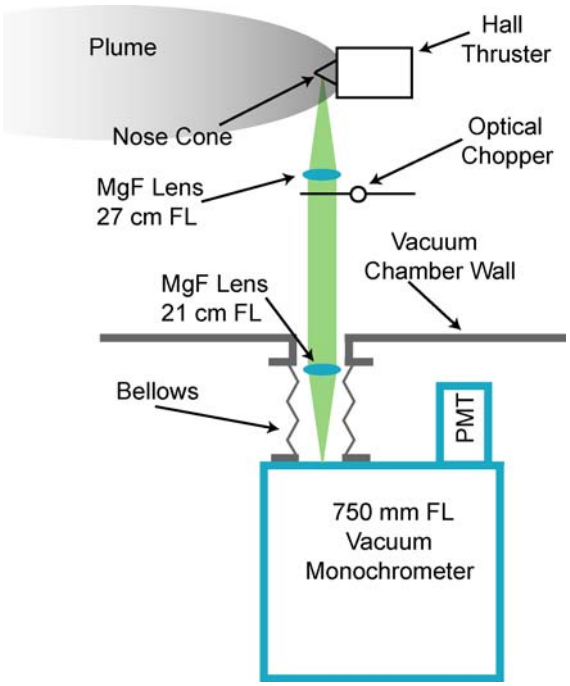

Fig. 2. Experimental apparatus for measurement of boron emission from the nose cone of a 200 W Hall thruster.

Optical Emission Measurements

Figure 2 shows a schematic of the optical emission measurement apparatus. Two magnesium fluoride (MgF_2) lenses (25 mm diameter) collect and focus the plasma emission. The lenses (27 and 21 cm focal lengths, respectively) focus the emission signal into an Acton Research 750 mm focal length (FL) vacuum monochrometer with a solar blind vacuum ultraviolet

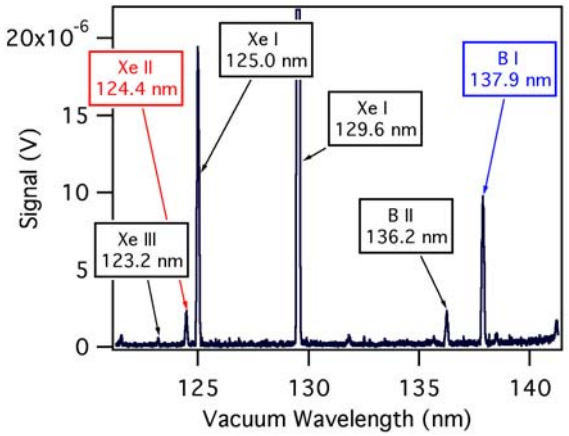

Fig. 3. Scan of spectral region of interest. Significant transitions of Xe and B are labeled.

(VUV) photomultiplier tube (PMT). The entrance and exit slits of the monochrometer (100 μm width, 6 mm height) were imaged on the thruster nose cone 4 mm from the thruster exit plane. The signal is chopped (330 Hz) using an SRS 540 optical chopper within the vacuum chamber for phase sensitive detection. All measurements were taken using an SRS 850 lock-in amplifier. For accurate placement of the thruster relative to the optical train, the thruster is placed on a three axis translation system within the vacuum chamber (not shown).

The VUV portion of the spectrum was chosen due to the easy identification and wide spacing between emission lines. Also, these electronic transitions are often closely coupled to the ground state and more representative of the bulk population than emission between excited states. The lines investigated in this study are the ionic xenon (Xe II) line at 124.4 nm and the neutral boron feature (B I) at 137.9 nm [2]. The B I feature is actually composed of four distinct transitions (137.87, 137.89, 137.89, and 137.92 nm) which are not resolved by the instruments. Figure 3 shows a spectral survey of the region of interest with the relevant lines identified. Note the rise in the baseline due to the strong Xe I transition at 147 nm.

LIF Ion Velocity Measurements

LIF measurements of Xe II velocity were taken of this thruster for conditions similar to those in Table 1. The only operational difference is that power was not supplied to the heater, or keeper. The spectroscopy and LIF measurement techniques are described more fully elsewhere [3-4].

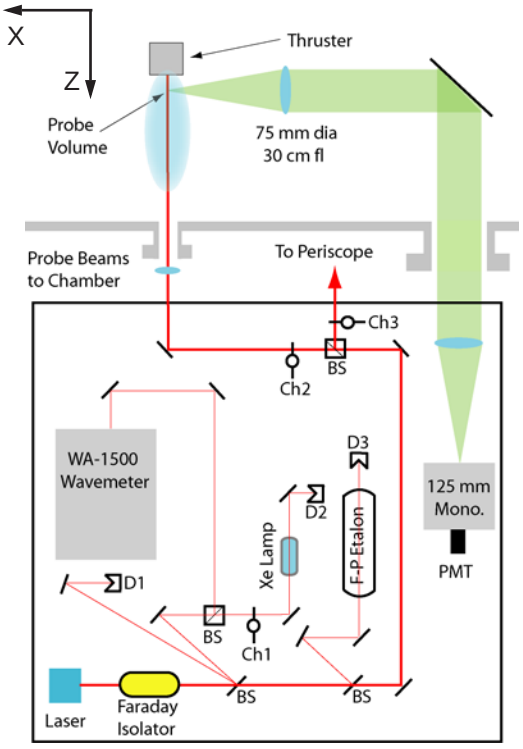

Fig. 4. Top view diagram of the laser optical train and collection optics. Note that the radial probe beam periscope and focusing optics are not shown.

Figure 4 shows a schematic of the LIF experimental apparatus. The thruster is mounted on a three axis orthogonal computer controlled translation system (not shown). The X-Z plane is shown in Fig. 4. (not shown is the orthogonal probe beam which provided the Y axis velocity component). The measurements in this work are limited to the Y-Z plane along the thruster line of symmetry, hence the Z and Y velocity components correspond to the axial and radial velocity componets.

A New Focus Vortex tunable diode laser, capable of tuning approximate ±50 GHz about a center wavelength of 834.7 nm, is used for these measurements. It is passed through a number of diagnostics and split into two probe beams each optically chopped at distinct frequencies (2.0 and 2.8 kHz). This allows for phase sensitive detection of the fluorescence signals using a single collection optics train and photomultiplier detector. Due to the magnification of the collection optics and detector entrance aperture, the spatial resolution of the measurements is 1 mm in the axial (Z) and 1.7 mm in the radial (Y) axes. Ion velocities are calcu-

lated by measuring the doppler shifted LIF signal relative to a stationary reference cell.

Plume Current Density Measurements

A molybdenum guarded Faraday probe measured the ion current flux exhausted by the cluster. The Faraday probe is a coaxial design with a central collector (19.1 mm diameter) and a guard ring (45 mm outer diameter) with an approximately 1.5 mm spacing. The current collection probe surfaces are mounted to a ceramic mount. The probe and guard ring are biased 30 V below chamber ground, approximately 18 V below the thruster hollow cathode potential which floated freely at approximately -12 V. The probe current is measured using an Agilent 34970A data acquisition and switch unit which allowed high resolution measurement of the collected ion current through an internal precision 5 Ω resistor. These probes have been used in previous measurements [1].

The probe is mounted on an arm 60 cm from the thruster nose cone tip. The arm is on a rotary stage that allowed the probe to rotate through the plume, ±90°. The probe and rotary schematic are shown in Fig. 5. No correction is made for secondary electron emission due to ion impact, or for multiply charged ions.

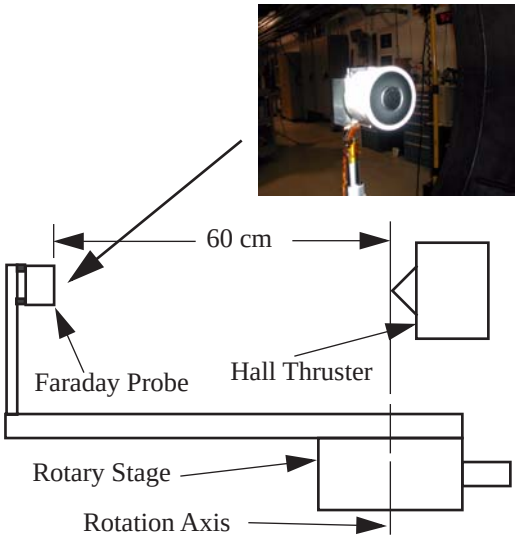

Fig. 5. Photograph of Faraday probe and schematic showing probe mounted on rotary translation system and position relative to Hall thruster

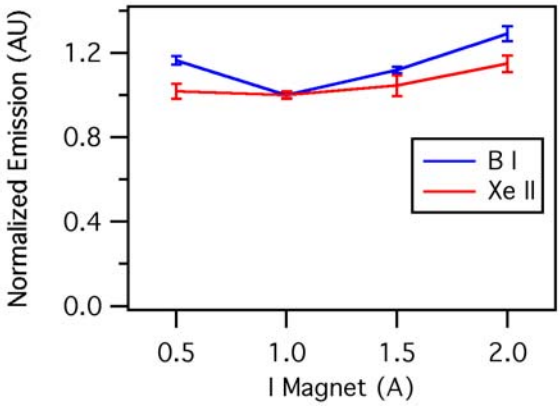

Fig. 6. B I and Xe II emission at nominal conditions with magnetic current (field) varied.

Experimental Results

Optical Emission Measurements

The optical emission measurement procedure consists of parking the monochrometer on the transition. The thruster operating conditions are then varied while the emission signal is recorded by the lock-in amplifier. The data are extracted by averaging the signal over a 100 second sample period. Uncertainties in the signals are determined from the standard deviation during the sampling period.

In all measurements, only one independent thruster control parameter (magnetic field, discharge potential, or propellant flow rate) is varied relative to the nominal operating conditions in Table 1. Emission values are normalized to those seen during nominal operation. Measurements of the B I emission at 137.9 nm and Xe II at 124.4 nm were performed in this way.

Figure 6 shows the variation of B I and Xe II emission as a function of current to the thruster magnetic circuit. The radial magnetic field varies approximately linearly with magnet current. With the magnet currents at 0.5, 1.0 (nominal), 1.5, and 2.0 A, the anode currents were at 770, 850 (nominal), 894, and 770 mA, respectively. Anode current was steady in all but the last case where the variation was significant, ±80 mA. For the cases with steady operation, the variation of anode current with magnetic circuit current is less than 10%.

Figure 6 shows that varying the radial magnetic field changes emission signal of B I significantly, while the emission of Xe II is not changed as significantly. This appears to indicate that the plasma is not significantly affected (i.e. temperature, density remain

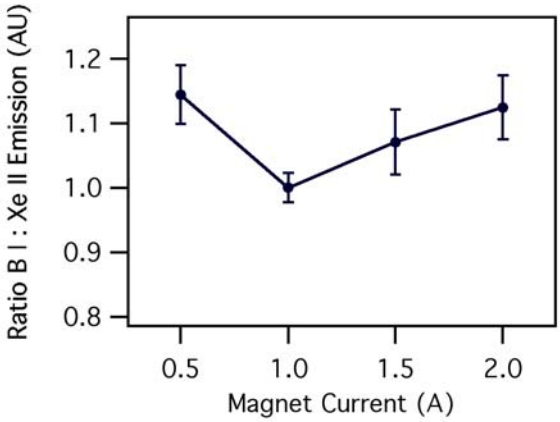

Fig. 7. Ratio of B I to Xe II emission with magnetic current (field) varied.

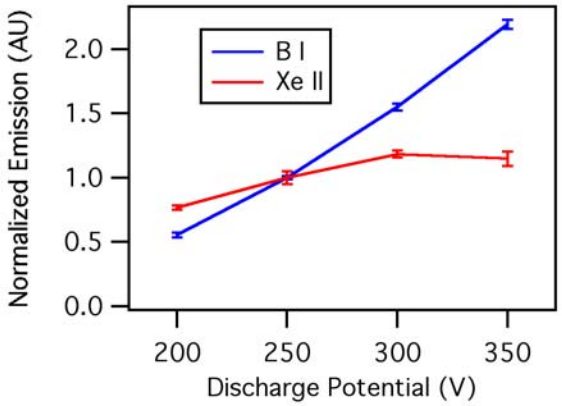

Fig. 8. B I and Xe II emission with discharge potential (electric field) varied.

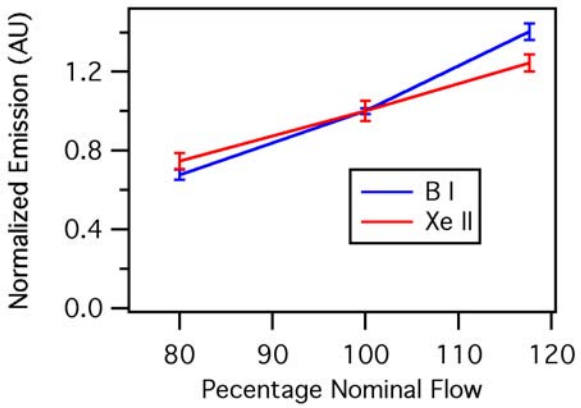

Fig. 9. B I and Xe II emission with propellant flow rate (plasma density) varied.

approximately constant), while the B I emission increases. Figure 7 shows the ratio of the B I to Xe II emission. It clearly shows a minimum in the ratio of emissions at nominal magnet current, but also in the magnitude of the low frequency (<0.1 Hz) oscillations as denoted by the emission signal uncertainty bands. It would appear that choosing an optimum magnetic field strength is not merely a function of minimizing the anode current. In this case, it appears that erosion of the thruster is also minimized by choosing an intermediate magnetic field where very low frequency (<0.1 Hz) emission, and hence plasma, oscillations are also minimized.

Previous measurements have shown that the length over which ions are accelerated within a Hall thruster does not vary with discharge potential [4]. Increases in the discharge potential directly translate into increases in the average electric field within the ion acceleration region. Increasing the discharge potential will produce more energetic, faster ions, thereby lowering the plasma density. Similarly, it may increase the electron temperature of the electrons which will in turn affect the energy distribution of the excited states of xenon. B I emission will not be directly affected on by the electric field. The lower state of the four B I transitions is the ground state. Hence, the B emission is unlikely to be in thermodynamic equilibrium with the electrons as one might expect of transitions between highly excited states [5]. It is therefore believed that B I emission is not significantly affected by these changes in the propellant plasma density and temperature.

Figure 8 shows B I and Xe II emission for discharge potentials of 200, 250 (nominal), 300, and 350 V. The anode currents for these cases are 810, 860 (nominal), 830, and 760 mA, respectively. All anode current values are within 12% of nominal and generally within 5% (except for the 350 V case). The B I emission rises linearly with discharge voltage. From the nominal discharge voltage (250 V), increases of 50 V appear to result in increases of 50% in B I emission. Extrapolation to zero B I emission yields a discharge potential between 140-160 V. Xe II emission also varies with discharge voltage to a lesser degree. The Xe II emission signal initially rises with the rising discharge voltage. At higher discharge potentials, it then levels and may decline.

Assuming the ionization fraction is unchanged, changing the propellant flow rate to the anode discharge will vary the plasma density. Figure 7 shows the resulting emission from the 80% nominal, 100% nominal, and 118% nominal flow rates. The anode currents for these cases were 675 (78% nominal), 860 (nominal), and 1,010 mA (117% nominal). The B I emission appears to rise linearly with rising propellant flow. Unsurprisingly,

so does the Xe II emission. Extrapolation to zero B I emission yields a propellant flow 10-15% of nominal.

Ion Velocity LIF Measurements

LIF xenon ion velocity measurements were taken in the region shown in Fig. 10. Eight points were interrogated at 1 mm intervals. The measurements are spatially resolved to 1 mm in the axial (Z) direction and 1.7 mm in the radial (Y) direction. The total uncertainty in the velocity measurements is approximately ±500 m/s. However, the measurements themselves have been shown to be repeatable to better than ±75 m/s. The LIF cases correspond to the majority of the measurement conditions of the emission measurements, and provide valuable insight into the effect of thruster conditions on plume divergence. LIF data for the nominal case, 0.5 A magnetic current, 200 V discharge potential, 300 V discharge potential, 80% nominal propellant flow, and 118% nominal propellant flow are available.

Figure 11 shows the flow angle calculated from the axial and radial velocity components. The flow angles are negative denoting the flow is diverging from the annular acceleration channel inward toward the thruster centerline. The most divergent case occurs when the magnet current is 50% of nominal. The flow is approximately 3° more divergent than the nominal case and 2° more divergent than the next worst case, 200 V discharge potential. The 300 V case is least divergent with a 2° decrease in divergence. Variation of the propellant flow rate does not appear to cause a significant change. However, the data imply that increasing the propellant flow, and hence the plasma density, will decrease the divergence slightly. Unfortunately, the small differences apparent in Fig. 11 are well within the uncertainty of the calculation of the flow angles and should be viewed with some caution.

Figure 12 shows the Xe II radial energy components calculated directly from the measured radial velocity. Nearest the exit plane, the radial energy of the xenon ions is approximately 10% of the discharge potential. This approximation holds for the nominal case as well as the 200 and 300 V discharge potential cases. Varying the propellant flow (plasma density) does not affect the radial energy significantly. However, the higher density case appears to have a higher ion energy normal to the insulator surface. This is consistent with the supposition that as the density within the acceleration channel increases, the likelihood of ion-heavy species collisions increases, producing greater flow divergence. The lack of consistency within Figs. 11 and

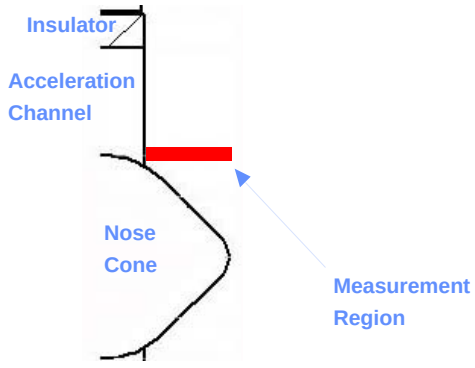

Fig. 10. Location of Xe II LIF velocity measurements relative to the nose cone. All measurements are referenced from the exit plane (left). The nose cone extends approximately 7 mm beyond the exit plane.

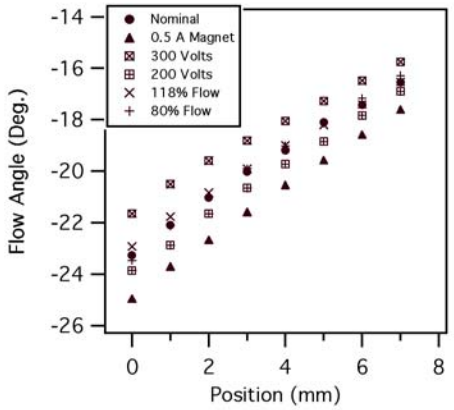

Fig. 11. Ion flow angles calculated from axial and radial velocity components measured via LIF for six operating conditions. Position is specified in distance from thruster exit plane.

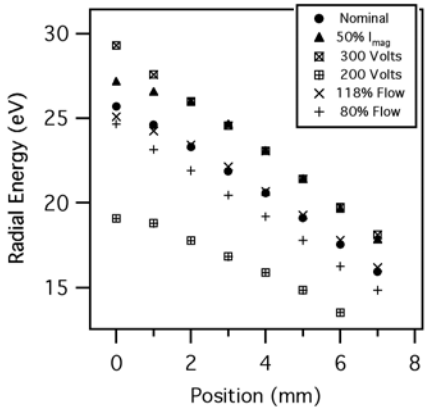

Fig. 12. Radial ion energies calculated from radial velocity components measured via LIF for six operating conditions. Position is specified in distance from thruster exit plane.

12 must take into account the greater uncertainty in calculating the flow angle compared to calculating the radial energy [6-7].

The influence of the magnetic field strength is also evident in Fig. 12. Here we see a 2-3 eV increase in the radial energy with a 50% decrease in magnetic field (this corresponds to 0.5 A versus the nominal 1.0 A magnet current) relative to the nominal case. Several millimeters from the exit plane, the reduced magnetic field case has the same energy as the 300 V discharge potential case. It appears that a non-optimal setting of the radial magnetic field will result in greater erosion simply due to increased radial energy of the ions. In Fig. 11, this is shown as a greater ion flow divergence.

Faraday Probe Plume Divergence Measurements

Faraday probe measurements of ion current flux were taken for most conditions examined by the B emission and LIF ion velocity measurements. The measured ion current flux profile was integrated to determine the total ion current. As a figure of merit, the width of the profile was estimated by using the full width at half maximum (FWHM). Direct comparisons these parameters appear to provide a reasonable measure changes in thruster performance and plume divergence.

Figure 13 shows the integrated ion current (±90°) and FWHM of the measured plume profile in the case where the magnetic field is varied between 0.5 and 2.0 A in 0.1 A increments. The measured ion current displays a local minimum at approximately 0.8 A magnet current, but the total variation is 6%. This is comparable to the variation in ion emission in Fig. 6. The plume profile FWHM increases with increasing with increasing magnetic field. However, the rate of increase is less above 1.5 A

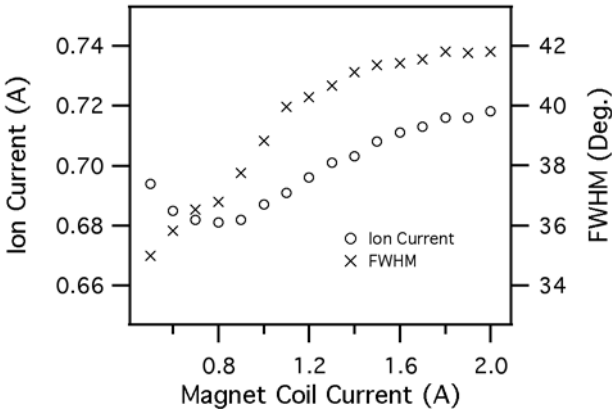

Fig. 13. Dependence of profile FWHM and integrated ion current on magnet coil current.

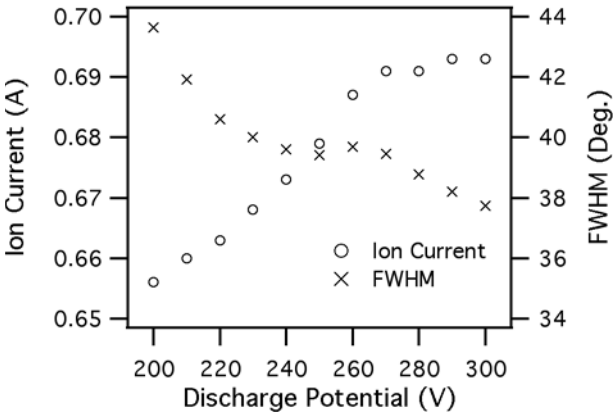

Fig. 14. Dependence of profile FWHM and integrated ion current on anode discharge potential.

Figure 14 shows the integrated ion current and FWHM of the measured plume profile in the case where the discharge potential is varied between 200 and 300 V in 10 V increments. Unfortunately, the Faraday probe measurements do not extend beyond a 300 V anode discharge potential. Here the measured ion current increases a total of 5% with increasing discharge potential. This change is similar to the behavior seen in Fig. 8 where the ion emission increases with increasing anode potential. However, increases in the ion current are significantly smaller. This indicates that the ion population distributions are likely changing. The plume profile FWHM decreases with increasing discharge potential. This behavior agrees with the behavior of the LIF flow angle measurements of Fig. 11.

Figure 15 shows the integrated ion current and FWHM of the measured plume profile in the case where the anode flow rate is varied between 85-118% of nominal in several increments. The ion current increases linearly as would be expected from the ion emission data in Fig. 9. In addition, the width of the plume profile is nearly unchanged. Total measured FWHM variation is less than 2°. However, it is interesting to note that the data suggests that increasing the propellent flow rate decreases the width of the plume slightly. This is similar to LIF flow angle data in Fig. 11, especially nearest the exit plane where the flow angle and radial ion energy data have the most relevance.

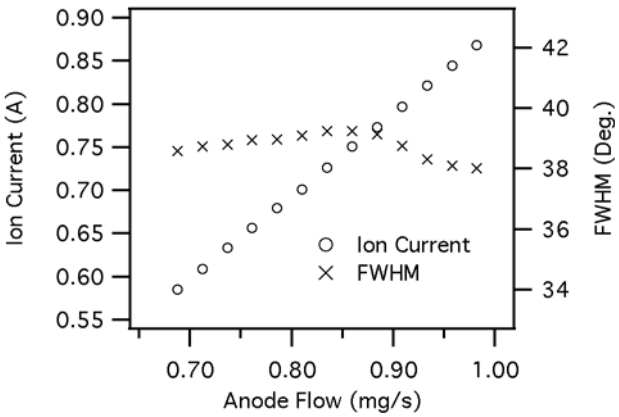

Fig. 15. Dependence of profile FWHM and integrated ion current on anode discharge flow rate.

It is important to note that the integrated ion current and FWHM of the plume profile should both be treated as figures of merit. Faraday probes such as the one used in this study appear to over predict the ion flux. Some of the possible causes include secondary electron emission, multiply charged species, and chamber back pressure [1]. The absolute accuracy of the measurements is questionable due to these issues. However, the precision of the individual measurements is better than 1% and trends are readily repeatable. Similarly, the ion current density profile FWHM is a convenient figure of merit due to the ease of calculation and reduction of uncertainties related to the extent of the high angle ion flux.

Analysis

Experimental Results

The accumulated data indicates that small changes in the control parameters of a Hall thruster have measurable effects on the signal strength of the B I emission, and hence the erosion rate of the BN insulator. This is further supported by the LIF and Faraday probe data. The clearest evidence is in Figs. 8 and 9 where the thruster operational and plasma parameters are nearly unchanged, but the B I emission (BN erosion rate) is strongly affected. This is verified by increased LIF measured flow divergence.

It is not unexpected that the magnetic field would have a strong effect on thruster operation. The magnetic field strongly affects electron conductivity which in turn generates the electric field within a Hall thruster. If the magnetic field is too strong and electron transport is severely impeded, the plasma will respond with high frequency oscillations (10-30 kHz) which seem to enhance electron conductivity. If it is too low, the discharge current will increase (and thruster efficiency falls) as more electrons reach the anode due to enhanced charge carrier mobility.

This strength of the magnetic field is also one of several factors which determines the location of the propellant ionization zone. The location where the propellant ionization occurs influences the propellant flow divergence, especially in the vicinity of the nose cone. If the ionization zone is shifted outward, the plume divergence increases due to the increased likelihood of divergent ions escaping the acceleration channel without impacting the walls. If the magnetic field strength is increased until it overly retards electron transport, plasma oscillations will locally increase plasma conductivity. This may also produce increased plume divergence due to longer ion drift times prior to significant axial acceleration. Both cases may reduce thruster lifetime by producing significant populations of radially divergent highly accelerated ions. The ideal case would appear to occur where ionization occurs over a short length scale in a strong electric field where the ions are created and accelerated prior to acquiring significant radial velocity.

In comparison, variation of propellant flow and discharge potential appear to have much simpler effects on insulator erosion. As a first order approximation, erosion rates are proportional to the ion flux. At the relatively low ion energies produced by a Hall thruster, sputter yields should vary linearly with ion energy. These hypotheses appear to be confirmed by the data in Figs. 6 and 7 which show B I emission to be linear proportional to both propellant flow and discharge potential. This conclusion is reinforced by the radial ion energies calculated from LIF velocity measurements in Fig. 10.

It is interesting to note that increased flow appears to decrease plume profile FWHM. This is confirmed by both LIF and Faraday probe measurements. This is an unexpected result since increased density presumably increases the probability of collisions and hence increased, rather than decreased, plume divergence. The Faraday FWHM data shows that this is the case initially, but there follows an abrupt change in the FWHN trend which then decreases plume divergence as the plasma density rises. The source of this behavior is not known. We speculate that the increased plasma density is increasing the plasma conductivity and adjusting the location of the ionization and acceleration regions within the discharge chamber.

The Faraday probe integrated current and plume divergence as denoted by the ion flux profile FWHM appear to support most of the B I emission and LIF data. Varying the magnetic field and discharge potential produced less than 6% total variation in the integrated ion currents. The changes in the profile FWHM correspond to the LIF flow field measurements. However, the LIF derived flow angle dependence on magnetic field do not correspond to changes seen in the Faraday probe measurements. It appears that this behavior is not captured by the Faraday probe. It must be remembered that the Faraday probe data provides a global view of the plume while the LIF data provides a decidedly local view of the flow field.

Sputtering Trends

Sputtering literature for compounds is limited. Sputter yields are highly dependent on energy, impact angle, and surface morphology. BN sputter yield literature are not believed to be available. However, certain Hall thruster trends can be inferred from our measurements and experience.

Erosion rate, E_r, is the product of the ion flux, F_i, and sputter yield, Y_s. The ion flux is proportional to the propellant flow, which is in turn proportional to the discharge current, I_d. In the low ion energy regime (<500 eV), the sputter yield is assumed to be proportional to the energy of the impacting ions, which is in turn proportional to the discharge potential, V_d (as shown by LIF data). It is thus possible to relate E_r to the product $I_d \cdot V_d$. This is equivalent to the thruster power, P_d.

$$E_r = F_i \cdot Y_s \sim I_d \cdot V_d = P_d$$

If it is implicitly assumed that the erosion processes do not significantly change during life, thruster life may be defined by a finite duration of erosion.

$$Life = \int E_r dt \sim \int P_d dt$$

Hall thruster lifetime is therefore proportional to the time integrated power of the discharge, or total energy dissipated by the anode discharge. This is an approximation which can be used to predict changes in lifetime based on small changes in operational parameters (e.g. flow rate and discharge potential).

Conclusions

This work has examined the emission of B I from a BN Hall thruster insulator to develop a diagnostic which allows for real time, in situ monitoring of insulator erosion. It is assumed that the B I emission signal is proportional to the sputter rate of the BN insulator. By examining at a number of off-nominal operating conditions, we show that insulator erosion appears to be linearly dependent on the discharge potential and the propellant flow rate. These measurements are supported by LIF measurements of Xe II velocity which show the radial ion energies proportional to the discharge potential. The velocity measurements also show the increase in divergence due to unoptimized magnetic field strengths which is confirmed by B I emission measurements.

Faraday probe measurements confirm that the thruster ion current is not significantly affected by the variation of the magnetic field or electric field. Changes in mass flow produce like changes in the ion current as the number of positive charge carriers is increased. Faraday probe measurements of the plume profile FWHM show that the divergence trends measured by ion LIF measurements for the most part propagate into the far field. The B I emission minimum evident with the variation of the magnetic coil current is partially confirmed by the LIF measurements, but this apparently local effect does not propagate downstream nor is evident in the Faraday probe measurements. This indicates that specialized measurements such as local ion velocity clarifies local plume behavior that are not evident by more global diagnostics.

The assumption that the B erosion can be measured by the B I emission signal strength alone is not completely rigorous. In these measurements where the erosion is occurring in what is essentially the near field plume, the assumption has some merit, but limitations become especially apparent when the discharge potential is varied. The ion population distributions appear to measurably vary, as a likely result of the changing electron temperature. It now becomes necessary to consider the application of a collisional radiative model to determine an improved estimate of the relative B densities as has been done by others [8].

Acknowledgements

The author would like to thank Professor Mark Cappelli of Stanford University for the loan and assistance with the use of the VUV monochrometer. Author J. Strafaccia was supported by an AFRL summer internship from the US Air Force Academy.

References

1. W. A. Hargus, Jr. and G. Reed, "The Air Force Clustered Hall Thruster Program," AIAA-2002-3678, *38th Joint Propulsion Conference*, 7-10 July 2003, Indianapolis, IN.
2. National Institute of Science and Technology (NIST) Atomic Spectral Data Base, NIST Standard Reference Database #78, *physics.nist.gov/cgi-bin/AtData/main_asd.*
3. W.A. Hargus, Jr. and C. S. Charles, "Near Exit Plane Velocity Field of a 200 W Hall Thruster," AIAA-2003-5154, *39th Joint Propulsion Conference*, 27-29 July 2003, Huntsville, AL.
4. W. A. Hargus, Jr. and M. A. Cappelli, "Laser-Induced Fluorescence Measurements of Velocity within a Hall Discharge," *Applied Physics B*, Vol. 72, pp 961-969, 2001.
5. H. R. Griem, *Plasma Spectroscopy.* McGraw-Hill Book Company, New York, 1964.
6. A. Jeffrey, *Handbook of Mathematical Formulas and Integrals*, Academic Press, Inc., San Diego, 1995.
7. J. R. Taylor, *An Introduction of Error Analysis: The Study of Uncertainties in Physical Measurements*, 2 Ed., University Science Books, Sausalito, CA, 1997.
8. D. Pagnon, P. Lasgorceix, and M. Touzeau, "Control of the Ceramic Erosion by Optical Emission Spectroscopy: Parametric Studies of PPS1350-G and SPT100-ML," *40th Joint Propulsion Conference*, 11-14 July 2004, Fort Lauderdale, FL